POLITECNICO DI TORINO
Repository ISTITUZIONALE

The Impact of Occupancy-Related Input Data Uncertainty on the Distribution of Building Simulation Results

Original
The Impact of Occupancy-Related Input Data Uncertainty on the Distribution of Building Simulation Results / Berger, Christiane; Primo, Elisa; Wolosiuk, Dawid; Corrado, Vincenzo; Mahdavi, Ardeshir. - ELETTRONICO. - (2020), pp. 1-6. (Intervento presentato al convegno Building Simulation Applications - BSA 2019 - 4th IBPSA-Italy conference tenutosi a Bozen-Bolzano nel 19th-21st June 2019).

Availability:
This version is available at: 11583/2846155 since: 2020-09-20T19:48:06Z

Publisher:
Bozen-Bolzano University Press

Published
DOI:

Terms of use:

This article is made available under terms and conditions as specified in the corresponding bibliographic description in the repository

Publisher copyright

(Article begins on next page)

21 September 2024

Manuscript
Click here to download Manuscript: Zeolite_water_protocol_revised.pdf Click here to view linked References

Protocols for atomistic modeling of water uptake into zeolite crystals for thermal storage and other applications

Matteo Fasano[a], Daniele Borri[a], Eliodoro Chiavazzo[a], Pietro Asinari[a,*]

[a]*Energy Department, Politecnico di Torino, Corso Duca degli Abruzzi 24, Torino, 10129, Italy*

Abstract

We report numerical protocols for describing the water uptake process into microporous materials, with special emphasis on zeolite crystals. A better understanding and more predictive tools of the latter process are critical for a number of modern engineering applications ranging from the optimization of *loss free* and compact thermal storage plants up to more efficient separation processes. Water sorption (and desorption) is indeed the key physical phenomenon to consider when designing several heat storage cycles, whereas water infiltration is to be studied when concerned with sieving through microporous materials for manufacturing selective membranes (e.g. water desalination by reverse osmosis). Despite the two quite different applications above, in this article we make an effort for illustrating a comprehensive numerical framework for predicting the engineering performances of microporous materials, based on detailed atomistic models. Thanks to the nowadays spectacular progresses in synthesizing an ever increasing number of new materials with desired properties such as zeolite with various concentration of hydrophilic defects, we believe that the reported tools can possibly guide engineers in choosing and optimizing innovative materials for (thermal) engineering applications in the near future.

Keywords: `Zeolite, Thermal storage, Water sorption, Water`

*Corresponding author
Email address: `pietro.asinari@polito.it` (Pietro Asinari)

infiltration, Microporous materials, Molecular dynamics, Monte Carlo

1. Introduction

In the last decades, the increase in worldwide human population, industrialization and technological development have been causing a growth in the use of fossil fuels, which in turn has increased greenhouse gas emissions and fuel prices [1]. Those events motivate a more extensive and efficient exploitation of the various renewable energy resources, such as solar, tidal, wind or geothermal technologies [2]. To this end, one of the major limiting factor is the mismatch between most renewable energy availability and user demand, which is particularly the case of solar energy due to its intrinsically intermittent and unpredictable nature [1, 3, 4]. Therefore, energy storage technologies can play an increasingly important role towards a better equilibrium between energy supply and demand, with the additional aim to make accessible everywhere and every time electrical and thermal power.

Particularly focusing on thermal energy, sensible [5] or latent [6] heat storage systems are the most studied and established solutions in the field. However, due to unavoidable energy losses, those approaches are often not suitable for long-term applications [7]. On the contrary, storage systems based on sorption phenomena show high energy density, negligible heat losses and allow repetitive storage operations [8]. Systems using water as sorbate present the additional advantages of no toxicity, low cost and large availability. In this context, zeolite materials are showing great potential for heat storage applications [1].

Zeolites are aluminosilicate materials that nowadays can be easily synthesized with a precise chemical composition and structure of the micropores [9]. The significant increase in the surface to volume ratio and the peculiar physical properties of water under nanoconfined conditions are the main motivations of the growing interest for zeolite materials in several fields [10, 11]. In fact, the increased solvent accessible surface area enhances the solid-liquid interactions,

which in turn modify the liquid transport properties due to nanoconfinement effects [12, 13]. Generally speaking, such effects are of interest in modern engineering as they can be exploited for finely tailoring mass and energy transport properties in next-generation devices [14, 15, 16].

In particular, zeolite crystals present both large heat of adsorption and the capability to accommodate a significant amount of water without noticeable structure degradation, thus allowing durable heat release/accumulation cycles, respectively [17, 18]. Zeolite sorbents are typically non-toxic and present low mass density [19] in addition to a relatively low desorption temperature: all these features make them materials of great interest in thermal science for both heating [20, 21] and cooling purposes [22, 23, 24].

However, while the nanometer size of zeolite pores allows the sorption process to take place with large surface to volume ratios (as a rule of thumb, a teaspoon of zeolite or MOF materials have a inner pore surface equal to the area of a football field [25]) thus with high energy densities, it also involves nontrivial nanoscale effects on the mass transport of water inside the nanopores, such as surface barriers, single-file diffusion and nanoconfinement [26, 27, 28, 29, 30].

Therefore, modeling of the above phenomena is a non trivial task and it can often be accurately accomplished only by resorting to detailed atomistic tools, namely Monte Carlo (MC) and Molecular Dynamics (MD). In Figure 1, the fundamental tool for linking atomistic results to the engineering level is schematically represented: the connection of those drastically disparate scales can be achieved by constructing the *water uptake isotherms*. In this work, atomistic numerical protocols are used to investigate on the mechanism of both water adsorption and infiltration into zeolites with different hydrophilicity thus enabling to fully construct those isotherms.

In the low-pressure regime (i.e. below the saturation pressure), curves in Figure 1 are typically referred to as adsorption isotherms, and along with the value of the isosteric (adsorption) heat, are sufficient to reconstruct the isosteric field in the Clapeyron diagram. The latter is a convenient tool for the thermodynamic optimization of thermal storage cycles [31].

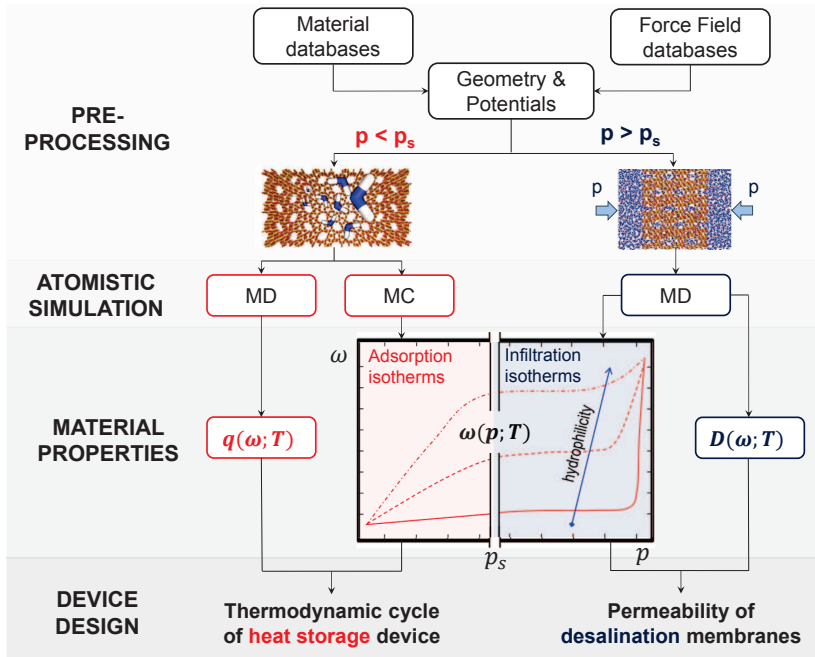

Figure 1: Protocols for the atomistic modeling by Molecular Dynamics - MD and Monte Carlo - MC methods of properties of nanoporous materials for thermal storage or desalination applications. Starting from the geometrical structure and force field, atomistic simulations are carried out to compute: (i) the isosteric heat $q(\omega;T)$ and adsorption isotherms $\omega(p;T)$, at $p < p_s$ (p_s being the saturation pressure); (ii) the infiltration isotherms $\omega(p;T)$ and the solvent diffusivity $D(\omega;T)$ for evaluating the membrane permeability, at $p > p_s$. Water uptake isotherms can be regarded as a convenient linking tool for bridging the disparate space and time scales between atomistic simulations and engineering applications. The reported protocol may support computational design of devices based on nanostructured materials, such as modern thermal batteries and desalination membranes.

On the other side, in the high-pressure regime (larger than tens or hundreds of bars), curves in Figure 1 are referred to as infiltration isotherms and those are relevant for water-solute separation processes such as desalination by reverse osmosis. In fact, it is worth noticing that microporous materials can be also used for manufacturing selective membranes.

To this respect, thanks to sub-nanometer pore sizes, excellent rejection rates are expected when using zeolite crystals, or other materials with a narrow pore

size distribution. Better selective membranes can indeed help in the near future in lowering the overall energy requirements in water desalination and other separation processes. The permeability of a microporous membrane depends on both the solubility coefficient, definable on the basis of the infiltration isotherms, (the more hydrophilic the more permeable) and the water mobility (diffusion coefficient, D) within the pores [12] (the more hydrophilic the less permeable). Given that it is *a priori* unclear which property (solubility or diffusivity) dominates the overall transport behavior [32], the right-hand side of Figure 1 represents an essential piece of information when it is to predict the membrane engineering performances.

In summary, computational materials design is a very promising research area, because it allows a more systematic investigation of novel materials for several applications [33]. This is particularly true for nanostructured materials, where macroscale properties are strongly affected by nanoscale characteristics and experiments are often limited by fabrication and visualization techniques, and thus multiscale modeling is needed [34]. In this article, we focus on numerical protocols in the form of a detailed sequence of atomistic modeling and simulation steps, as briefly sketched in (Figure 1), aiming at computing the main material properties needed when evaluating engineering performance of zeolite-based devices.

While different applications involve operating conditions with disparate pressure values, we suggest a comprehensive simulation framework for describing both adsorption and infiltration regimes. It is also recognized that reporting results in the form of adsorption isotherms, the latter represent a formidable tool for coping with the multiscale nature of the addressed problem, thus effectively linking atomistic details to more macroscopic properties and performances of engineering devices. Here, we take advantage of recent development of user-friendly software packages, such as GROMACS and Music. We hope that the reported tool can help the process towards a more rational design of novel nanoporous materials with tailored water uptake properties for both heat storage and water separation applications.

This manuscript is organized in sections as follows. In the Section 2, the adopted numerical protocols for modeling both adsorption and infiltration phenomena are described in detail. Examples of atomistic simulations of water adsorption into hydrophilic zeolite crystals and water infiltration into MFI defective zeolite are presented in Section 3. Finally, conclusions are drawn in Section 4.

2. Methods

Two modeling protocols based on atomistic simulations are here detailed, with the aim to numerically predict adsorption and infiltration phenomena of water intruded in zeolites for thermal storage and water separation applications, respectively.

First, a hybrid MD/MC protocol is designed to investigate both adsorption isotherms and isosteric heat of adsorption of water in a sample of 13X zeolite. This type of zeolite is typically adopted for thermal storage applications due to its hydrophilic behavior [35]. The geometry and force field of the simulated configuration, as well as a simulation protocol are required to perform atomistic simulations.

13X zeolite has a FAU structure with an Al/Si ratio of $1 \div 1.25$ and a number of Na cations equal to the amount of aluminum atoms and distributed in a few possible sites within the crystal [36]. The adsorption properties of zeolite are strongly influenced by both the amount of cations and their positions within the framework [36, 37]. As a representative example, a 13X zeolite with 76 Na cations per unit cell is here considered (leftmost picture in Figure 2) [38, 39]. Starting from the atomistic coordinates observed by NMR experiments [36], the initial amount of aluminum atoms in the 13X unit cell is modified to the target value. The substitution of Si atoms by Al ones is operated following the Lowenstein's rule. Cations are then randomly placed within the framework, while considering the possible occupancy sites [40] and avoiding energy peaks within the structure. The obtained unit cell is then replicated along x, y, z axes

in order to obtain a cubic simulation domain with 5.02 nm edge (2x2x2 unit cells).

The force field adopted for the MD/MC adsorption simulations takes into account bonded (i.e. covalent bonds) and nonbonded (i.e. van der Waals and Coulomb forces) potentials. The zeolite framework is considered fixed in the Monte Carlo simulations, whereas it is restrained by an harmonic potential in the Molecular Dynamics computations. Such assumption has been made to increase the simulation speed, and it does not significantly alter the adsorption properties of zeolite [41]. Note that no position restraints are applied to the Na cations, which are free to diffuse within the framework. Nonbonded interactions are mimicked by 12-6 Lennard-Jones (LJ) and Coulomb potentials, respectively. LJ parameters and partial charges for 13X zeolite are taken from Reference [38]. TIP4P is adopted as water model [42], coherently with similar studies in the literature [38].

Given geometry and force field for the sorbent-sorbate couple to be tested, the simulation box is first energy minimized with a steepest descent algorithm [43]. Then, adsorption isotherms are obtained by MC simulations, whereas heat of adsorption by MD ones (see Figure 2).

Equilibrium quantities are obtained through a series of Gran Canonical Monte Carlo simulations (GC-MC). MC simulations are carried out with up to 2 millions iterations, periodic boundary conditions along x, y, z axes, temperatures and pressures ranging from 300 to 350 K and from 10^{-4} to 3.5 kPa, respectively.

The isosteric heat of adsorption is instead obtained by MD runs. Starting from the equilibrated system, multiple configurations are generated by randomly inserting a controlled amount of water molecules in the zeolite pores, in order to evaluate the effect of pores hydration on heat of adsorption. Here, the considered hydration levels range from 5 to 100% of the water uptake at the saturation pressure (3.5 kPa), as computed by MC simulations. After the water molecule insertion, the velocities in the system are initialized by a Maxwell distribution at 300 K. The system is then relaxed to the target temperature (300 K) with

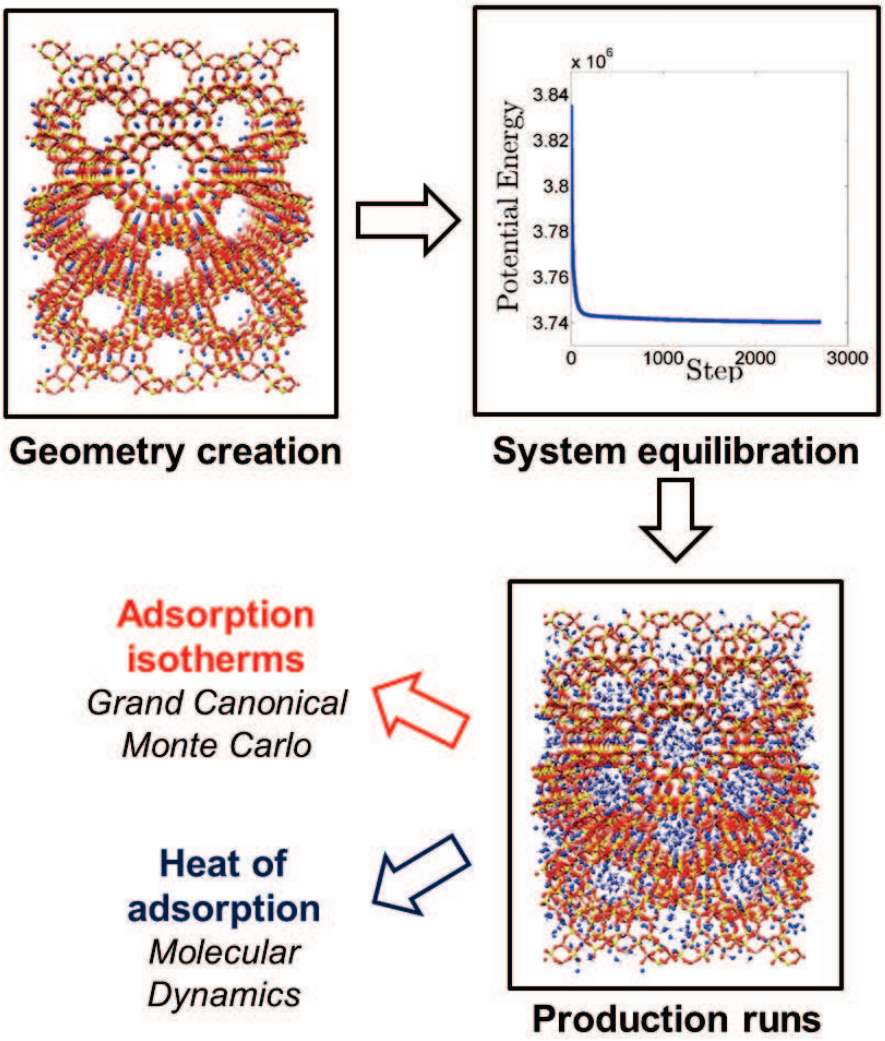

Figure 2: Simulation protocol adopted to study the adsorption phenomena of water in 13X zeolite. From left to right: once the geometry and force field of the zeolite framework are defined, the simulation domain is equilibrated and production run performed. Gran Canonical Monte Carlo allow to compute the adsorption isotherms of the considered sorbent-sorbate couple, whereas Molecular Dynamics the isosteric heat of adsorption.

a 1 ns MD simulation in NVT ensemble (Berendsen thermostat applied to the whole system [44]). After the thermalization step, the MD production runs are

carried out for up to 2 ns in NVT ensamble (Nosé-Hoover thermostat applied to the zeolite framework [45]). Heat of adsorption is computed from the average sorbate-sorbent (nonbonded) interaction energies during the simulated trajectory. Note that the simulated MD trajectories would also allow to compute the transport properties of water molecules intruded in the zeolite pores, such as viscosity, Fick's and self-diffusion coefficients.

Second, a MD protocol is developed to compute the infiltration isotherms of water in a sample of MFI zeolite, which is a zeolitic material currently investigated for reverse osmosis membranes with enhanced permeability and near 100% ions rejection [10].

This MD setup is designed for estimating the equilibrium water filling of a x, y periodic membrane at different solvent pressures, thus allowing to obtain the characteristic water infiltration isotherms of the tested material. The membrane is made out of either pristine (hydrophobic) or defected (hydrophilic) MFI zeolite (2x3x3 crystal cells), and it is restrained in the center of the simulation box. The membrane is then solvated in a large water box (about 30000 molecules are typically added, see Figure 3a), whereas the water-zeolite interface normal to z axis is functionalized by silanol terminals.

The force field adopted for the infiltration experiments takes into account both bonded and nonbonded interactions. Bonded interactions in the MFI crystal are modeled by both stretch and angle harmonic potentials. Parameters of the bonded interactions are reported elsewhere [46]. Nonbonded interactions between zeolite and water are crucial for defining the infiltration characteristics of the studied material [47, 48]. Here, van der Waals interactions are modeled by a 12-6 Lennard-Jones potential; partial charge interactions between solid surfaces and water are modeled by a Coulomb potential. Initially, both LJ and partial charges of MFI zeolite are taken from the values reported by Cailliez *et al.* [47], where partial charges of silicon, oxygen and hydrogen atoms in the MFI structure are $q_{Si} = 1.4$ e, $q_O = -q_{Si}/2$ and $q_H = q_{Si}/4$, respectively. The value of q_{Si} is successively tuned in order to better mimic experimental infiltration isotherms. TIP4P water model is adopted for the solvent [49], because

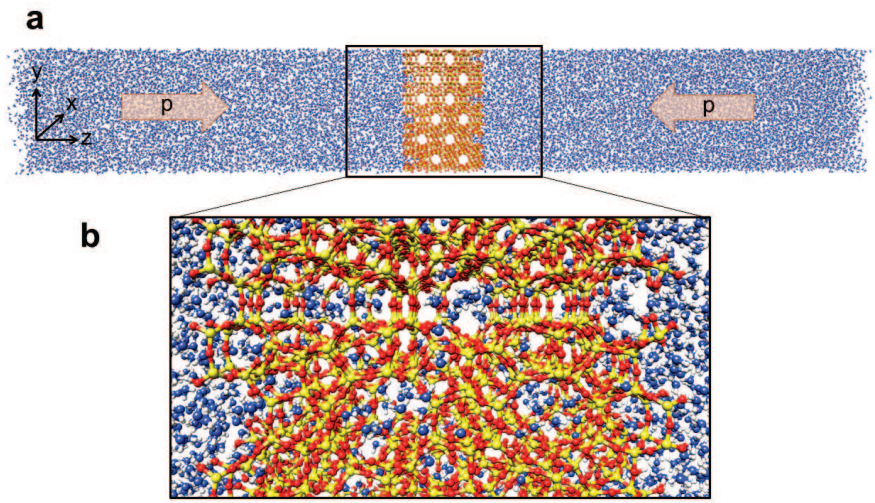

Figure 3: Simulated configuration for infiltration experiments. (a) Schematics of the MD simulation box: MFI zeolite membrane (red/yellow) and water molecules (blue) are represented. (b) MFI zeolite membrane after the water infiltration with p solvent pressure.

it well reproduces the transport properties of water molecules confined in MFI zeolite [47]. Intramolecular interactions of water molecules are fixed by LINCS algorithm [50], in order to increase the simulation timestep.

After that geometry is energy minimized, system velocities are initialized by a Maxwell distribution (300 K). System temperature is then equilibrated at 300 K and water pressure stabilized around 0.1 MPa by successive NVT and NPT runs, where Berendsen thermostat and barostat are used. Finally, infiltration runs are performed in NPT ensemble (velocity rescaled Berendsen thermostat with T=300 K; isotropic Parrinello-Rahman barostat with p water pressure to be tested), so that water molecules can intrude in the initially empty zeolite membrane until equilibrium conditions are reached (Figure 3b), typically after 10–35 ns. *In silico* infiltration experiments are performed in the pressure range 1-250 MPa, and only water molecules in the central portion of the membrane are considered as infiltrated, in order to avoid artifacts due to the broken crystallinity at the solid-liquid interface. Up to three repetitions per simulation with different initial conditions are performed and results averaged, for better

statistics. Kinetic end potential energies as well as pressure are checked for convergence during the simulation.

MC simulations are carried out by means of MUSIC [51], whereas MD ones by GROMACS [43] software. Rendering pictures are made with UCSF Chimera [52]. Lennard-Jones potentials are treated with a twin-range cut-off modified by a shift function (1.0 nm cut-off distance), whereas the Particle-Mesh Ewald (PME) algorithm [53] with 1 nm real-space cutoff and 0.12 nm reciprocal space gridding is chosen for electrostatic interactions. MD simulations are performed with a leap-from algorithm and time step $\Delta t = 2$ fs. Long range dispersion corrections are applied to avoid energy artifacts.

3. Results

3.1. Adsorption experiments

The presented simulation protocols may be adopted to study equilibrium and transport properties of fluids within a broad selection of microporous materials, e.g. zeolites, MOF or porous carbon materials. For demonstrating the robustness of the protocols, a few case studies are here reported: 13X and MFI zeolites, which are typically studied for heat storage and water filtration applications, respectively.

First, adsorption isotherms of water in 13X zeolite (76 Na) are obtained from Monte Carlo simulations at different temperatures, namely $T = 300$, 325, 350 and 375 K (Figure 4a). Given temperature and pressure, Monte Carlo simulations allow to compute the water uptake ω, which corresponds to the equilibrium amount of adsorbed water molecules per unit cell (N/UC). Note that ω can be easily expressed into more engineering measure units, such as mass of water per mass of zeolite (i.e. the load $\mathrm{kg_W/kg_Z}$), by considering the water (M_W) and zeolite's unit cell (M_Z) molar mass: $[kg_W/kg_Z] = [N/UC]\, M_W/M_Z$.

Coherently with similar hydrophilic zeolites analyzed in the literature [38, 54], the simulation results (symbols in Figure 4a and b) show a typical type-I adsorption behavior, which can be fitted by Toth equation for heterogeneous

systems (solid lines):

$$\omega\left(p,T\right)=\frac{Ap}{\left[1+\left(Bp\right)^{m}\right]^{1/m}}, \tag{1}$$

being $A=\omega_m B$ and ω_m the maximum adsorbed amount, B the Toth adsorption constant, which is related to the Henry law slope, and m the heterogeneity parameter [54]. Note that $m=1$ reduces Equation 1 to Langmuir sorption isotherm, whereas the heterogeneity of the sorbent-sorbate system enhances m deviation from 1. Simulation results are accurately ($R^2>0.93$, see the residual plot in Figure 4b) fitted to Equation 1 by an optimization procedure based on genetic algorithm. Similarly to the experimental results by Wang and LeVan [55], the obtained Toth equation parameters show coherent variations with temperature, namely:

$$A(T)=A_0\exp\left(E/T\right), \tag{2}$$

$$B(T)=B_0\exp\left(E/T\right), \tag{3}$$

and

$$m(T)=m_0+C/T. \tag{4}$$

In detail, Equations 2 and 3 are best fitted by $A_0=1.84\times10^{-1}$ kPa^{-1}, $B_0=3.57\times10^{-4}$ kPa^{-1} and $E=7585$ K ($R^2=0.99$), namely a exponential decrease of Toth adsorption constant with temperature. On the other hand, Equation 4 is best fitted by $m_0=2.52\times10^{-2}$ and $C=29.6$ K ($R^2=0.8$), namely a slightly decreasing trend of heterogeneity parameter. Therefore, water uptake decreases at high temperature, because of the exothermic nature of water adsorption to 13X zeolite. Results in Figure 4 also show that the most of water uptake, takes place at low pressures (approximately $p<0.1$ kPa and it increases with T), whereas only marginal further uptakes can be noticed in the remaining adsorption range. Hence, the former pressure range should be considered for determining the conditions needed to regenerate thermal batteries based on the simulated 13X zeolite.

MD simulations are then carried out to estimate the isosteric heat of adsorption (q) of the sorbent-sorbate couple considered so far, namely the enthalpy

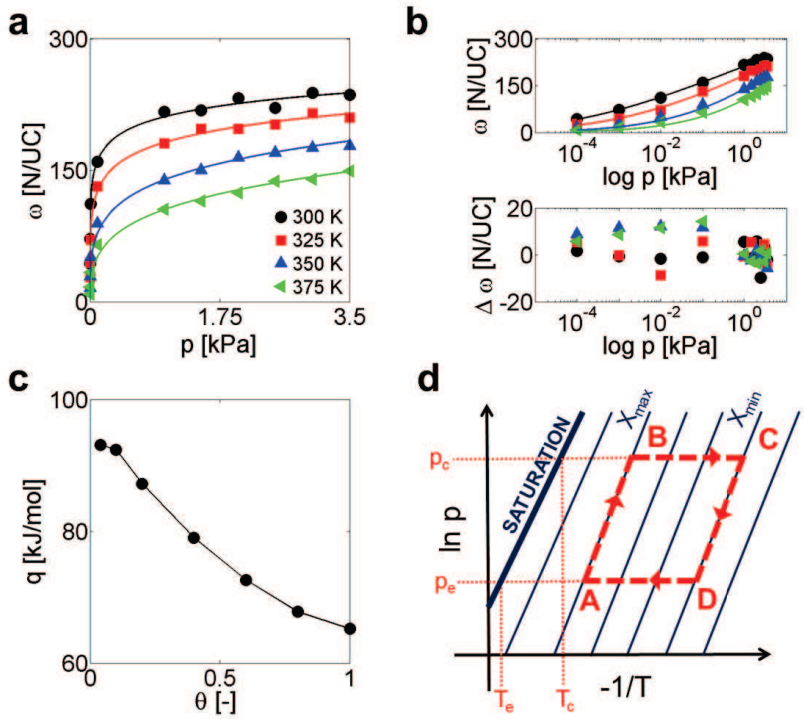

Figure 4: Atomistic simulations of water adsorption in 13X zeolite (76 Na) for heat storage applications. (a) Adsorption isotherms at different temperatures: MC results (symbols) vs. Toth equation fitting (solid lines, Equation 1). (b) To better visualize adsorption isotherms at low p, pressures are reported in a logarithmic axis (upper panel). Moreover, the residuals between MC results and Toth model fitting are plotted (lower panel). (c) Heat of adsorption at different hydration levels (θ). (d) Ideal cycle for a heat storage device based on sorption phenomena, represented on the isosteric field in the Clapeyron diagram.

(ΔH) released by the sorbate during the adsorption process. The analysis is only performed at 300 K, because q is only slightly temperature dependent. Different techniques allow to calculate q from atomistic simulations [56]. Neglecting the kinetic energy contribution to q (i.e. low T, as in the typical thermal storage applications), it is possible to demonstrate that

$$-q = \Delta H \approx U_{WZ} - U_{WW}, \tag{5}$$

where U_{WZ} and U_{WW} are the sorbent-sorbate and sorbate-sorbate interaction energies. Here, U_{WZ} and U_{WW} correspond to the average water-zeolite

and water-water nonbonded interaction energies, which can be easily extracted from the MD trajectories. Results in Figure 4c show that q decreases with the nanopores hydration, in good agreement with previous experimental and modeling studies [38]. In fact, the first molecules adsorbed to the nanopore surface can fully lie in the water-zeolite potential well, therefore releasing a larger part of their kinetic energy. Instead, successive adsorbed molecules progressively experience a screen effect from the first ones, therefore causing a smaller enthalpy release and thus lower q.

Adsorption isotherms and isosteric heat of adsorption are the fundamental properties of a sorbent-sorbate couple to be estimated in order to design the working cycle of sorption heat storage devices. An ideal water sorption heat storage system realizes an inverse cycle which can be conveniently illustrated in the Clapeyron diagram, as sketched in Figure 4d. The heat of adsorption can be determined using the Clausius-Clapeyron equation [57], namely $\left(\frac{\partial \ln p}{\partial -1/T}\right)_X = \frac{q}{R}$, which represents a set of isosters in the Clapeyron diagram and can be determined by the adsorption isotherms of the chosen sorbent-sorbate couple. Starting from a fully adsorbed thermal battery (A point in Figure 4d), the sorbent may be heated along an isosteric curve (A-B). A further heat supply to the sorbent (B-C) causes the desorption of the sorbate at (ideally) constant pressure (p_c, condensation pressure), thus being responsible for the regeneration of the thermal battery. Unlike standard inverse cycles, sorption heat storage cycles are interrupted (at C) for allowing heat conservation. A change in the ambient conditions (e.g. seasonal heat storage) can then decrease the system temperature without further molar changes (C-D). Finally, the key process is the heat released along the discharge path D-A at constant evaporation pressure (p_e), which takes place when sorbent and sorbate are put in contact. The heat released can be computed as $Q_{D-A} = \left|\int_{X_{min}}^{X_{max}} q\left(X, T(X), p_e\right) dX\right|$. Note that A and C points are defined by the working conditions of the system, whereas B and D depend on the selected sorbent-sorbate couple, which determines the equation of the set of isosteres. Hence, accurate modeling tools for predicting sorbate adsorption into a broad variety of sorbent are critical for a more rational

design of sorption thermal storage systems.

3.2. Infiltration experiments

Equilibrium and transport infiltration properties of water confined within nanopores are determined by geometric (i.e. pore size and network), physical (i.e. pore filling, temperature, pressure) and chemical (i.e. solid-liquid non-bonded interactions) factors [28]. In particular, the affinity between zeolite matrix and water (i.e. hydrophilicity degree) can be controlled by introducing hydrophilic defects in a pristine hydrophobic framework, thus precisely tuning the properties of the intruded water. For example, while pristine MFI zeolite (also known as silicalite-I) shows hydrophobic behavior, the introduction of aluminum defects fosters the creation of silanols (i.e. SiOH) thus a progressive increase of the hydrophilicity of the nanoporous framework [32]. Here, water infiltration in MFI zeolites with tunable hydrophilicity is studied by MD.

In the MD runs, steady state is considered as achieved when the water uptake ω converges to a constant value (Figure 5). This corresponds to the amount of water molecules in thermodynamic equilibrium with the system's chemical potential (i.e. pressure). First, the infiltration isotherm of water in silicalite-I obtained from MD simulations is compared with the experimental results presented in Reference [9]. Partial charges of the zeolite structure are then tuned for mimicking the experimental infiltration pressure ($\cong$ 100 MPa [9]): starting from the value suggested by Cailliez *et al.* (q_{Si} = 1.4 e, where e is the electron charge), MD runs show that q_{Si}=1.8 e better reproduces the experimental infiltration pressure of the considered silicalite-I membrane (Figure 6).

Note that the maximum framework infiltration capacity (ω_M) of the simulated structure is larger than the experimental evidence reported by Humplik *et al.*, namely 52 N/UC vs. 35 N/UC, respectively [9]. However, similar values have been found in other experimental (i.e. 53 N/UC [58]) and numerical studies (i.e. 57 N/UC [59]). Such discrepancy with experiments may be due to the analysis of imperfect zeolite specimens, which may present surface bar-

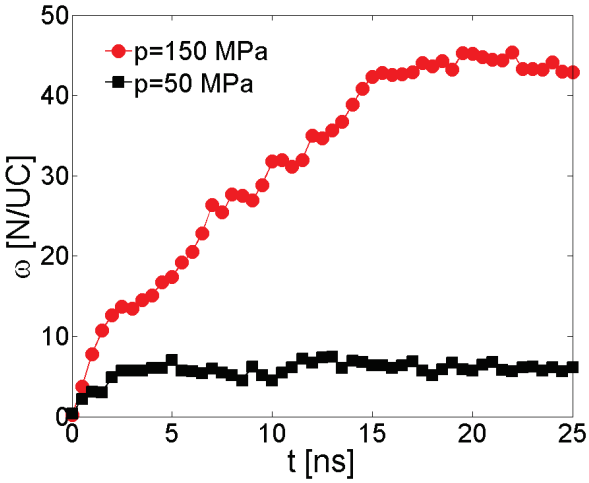

Figure 5: Water uptake ω in a silicalite-I membrane, at $p = 50$ (black squares) or 150 (red circles) MPa.

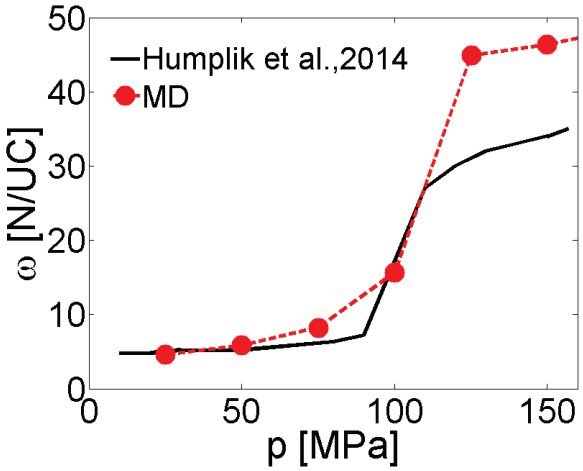

Figure 6: Infiltration isotherm of water in a silicalite-I membrane. Results from current MD simulations (red dots and dashed line) are compared with the experiments reported by Humplik *et al.* (black line) [32].

riers, pore blockage or contamination of the structure thus modifications of the accessible pore volume. On the other hand, numerical results may be affected by non-optimized force field parameters, such as water model or Lennard-Jones

coefficients. For the sake of completeness, while water model is kept constant in the following simulations, the effect of Lennard-Jones parameters on ω_M has been investigated. In particular, the inter-particle distance at which the LJ potential is zero for the oxygen atoms of the MFI zeolite is varied (σ). Starting from the base case (i.e. $\sigma = 0.30$ nm [47]), σ is increased up to 0.42 nm and the water uptake ω_M at $p = 250$ MPa evaluated by MD simulations. Considering a silicalite-I membrane, Figure 7 shows that ω_M decreases as σ increases. Therefore, the ω_M decrease is due to the reduction of water accessible volume in the zeolite's nanopores. However, changes in ω_M do not affect the dependence between infiltration pressures (i.e. infiltration type) and structure hydrophilicity [32], which is the focus of the following analysis.

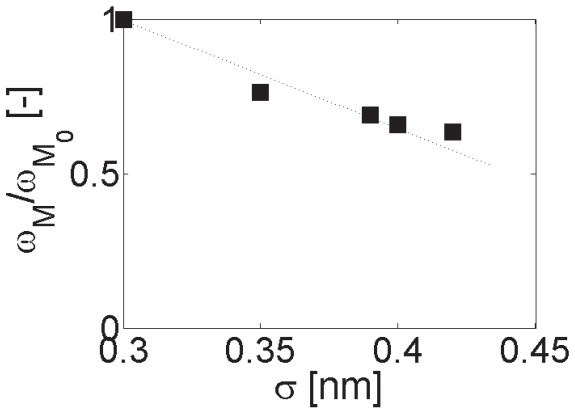

Figure 7: Influence of σ Lennard-Jones parameter for the oxygen atoms of silicalite-I membrane on the maximum framework infiltration capacity ω_M. Results are scaled by the framework capacity ω_{M0} of the base case, namely the case with $\sigma = 0.30$ nm. The black dotted line is a linear fitting of MD results.

After the preliminary tuning of the zeolite force field on experimental results, hydrophilic defects are introduced in the pristine structure, in order to study the infiltration behavior of water in hydrophilic MFI membranes. Here, defects mimic the substitution of silicon atoms by aluminum ones, which induces the creation of four local silanol nests [47]. A setup with 3.06% Al substitutions respect to the total amount of Si atoms in the structure (%Al/Si) is then

simulated.

Results in Figure 8 show that a small increase in the defect concentration (i.e. structure hydrophilicity) induces a dramatic change in the infiltration isotherm shape, coherently with experimental evidences and previous modeling works [32, 47]. MD results are then fitted by Dubinin-Astakhov equation (D-A), which is a model widely adopted for interpreting the dynamics of adsorption-infiltration processes [60]:

$$\frac{\omega - \omega_m}{\omega_M - \omega_m} = \exp\left[-\left(\frac{-k_B N_A T}{E_{DA}} \ln \frac{p}{p_M}\right)^{n_{DA}}\right]. \tag{6}$$

In Equation 6, p_M is the pressure at which ω_M is reached; E_{DA} and n_{DA} are D-A parameters related to the water-structure interaction energy and structure geometry, respectively; k_B is the Boltzmann constant, N_A the Avogadro number and T the system temperature. While ω_m, ω_M and p_M are known quantities, E_{DA} and n_{DA} are fitted to MD results. Here, the zeolite structure is assumed as invariant in the simulated setups thus n_{DA} constant, whereas E_{DA} related to defect densities. By means of optimizations based on genetic algorithm, $n_{DA} = 3.14$ is found to be the most accurate D-A exponent for the simulated MFI membranes. The optimized E_{DA} values are 2.30 and 3.85 KJ/mol for the pristine and the defected MFI zeolite, respectively. Figure 8 shows that D-A model (Equation 6) accurately fits ($R^2 > 0.90$) the obtained MD infiltration isotherms. As expected, the energy parameter E_{DA} increases with defect concentration, because the larger amount of hydrophilic spots in the structure implies higher interaction energies between the membrane and the intruded water molecules. Note that ω_M is independent from defect concentration, because it is only determined by the solvent accessible volume of the nanoporous structure.

The infiltration isotherm is clearly type-V in silicalite-I (according to IUPAC classification), which means that the membrane has an overall hydrophobic behavior. In this case, no infiltration occurs at low pressures, because bulk liquid-liquid interactions are stronger than the solid-liquid ones. Therefore, water condensation is dominated by liquid-liquid interactions at the infiltration

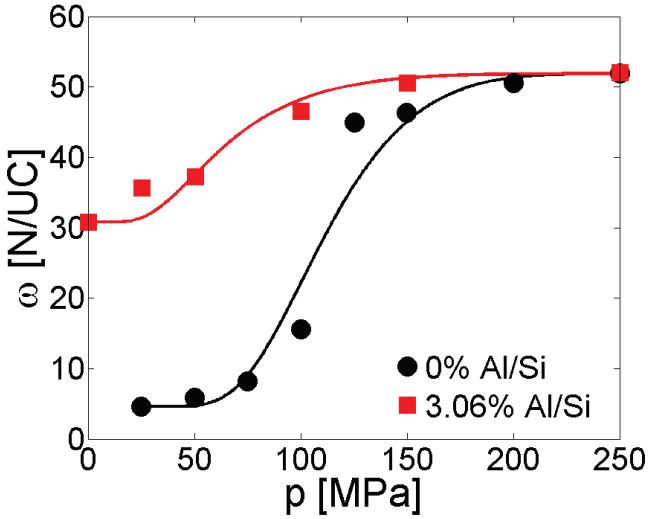

Figure 8: Infiltration isotherms of water in MFI zeolites with different defect densities: MD results (symbols) vs. D-A fitting (solid lines).

pressure, meaning that the condensation process starts with the homogeneous nucleation of water molecules and it is then followed by the collapse of the water clusters into the bulk liquid phase at the infiltration pressure [47, 48, 61]. The defect introduction within the MFI framework transforms the infiltration isotherm from type-V to type-I. In this case, solid-liquid interactions become dominant in the condensation process, thus inducing a heterogeneous nucleation of water molecules in the proximity of the most hydrophilic (i.e. defected) regions of the membrane [47, 58, 62, 63].

These numerical results demonstrate that small concentration of hydrophilic defects can significantly alter the infiltration characteristics of hydrophobic nanoporous materials, by enhancing their water uptake at infiltration pressures [32, 47]. On the contrary, some recent experimental studies have shown a significant increase in the transport of water in nanometer-sized hydrophobic pores [32]. Hence, since the overall permeability of membranes depends on both equilibrium (i.e. membrane solubility) and transport (i.e. water diffusivity) infiltration quantities, MFI zeolite may represent an ideal platform for a model-driven

design of the optimal defect concentration - thus hydrophilicity - of microporous materials for reverse osmosis applications.

4. Conclusions

In this article, numerical protocols for atomistic modeling of both water adsorption and infiltration into zeolite crystals have been presented. Those tools are essential for predicting the engineering performances of new promising materials of interest for thermal storage and water-solute applications. The essential tool for bridging the gap between atomistic simulation results and engineering level applications are the water uptake isotherms. On one side, in the low-pressure regime, the water adsorption isotherms (along with the knowledge of the isosteric heat) allows to perform thermodynamic optimization of sorption thermal storage cycles. On the other side, in the high-pressure regime, the water infiltration isotherms provide important information about the permeability of zeolite-based selective membranes. Better selective (and robust) membranes may help in the near future in lowering the overall energy consumption in water desalination and other separation processes. To this respect, as an example, it is shown that the introduction of hydrophilic defects within an originally hydrophobic nanoporous material is a possible approach for controlling the characteristic infiltration isotherms: starting from a hydrophobic structure (i.e. silicalite-I), the hydrophilicity of the zeolite membrane is then tuned by defect concentration.

Competing interests

The authors declare that they have no competing interests.

Acknowledgments

Authors are grateful to MITOR project (Compagnia di Sanpaolo) for travel support. PA, EC and MF would like to acknowledge the NANO-BRIDGE

– Heat and mass transport in NANO-structures by molecular dynamics, systematic model reduction, and non-equilibrium thermodynamics (PRIN 2012, grant number 2012LHPSJC) and the NANOSTEP – NANOfluid-based direct Solar absorption for Thermal Energy and water Purification (Fondazione CRT, Torino) projects. MF acknowledges travel support from the Scuola Interpolitecnica di Dottorato - SCUDO. Authors thank the CINECA (Iscra C project COGRAINS) and the Politecnico di Torino (DAUIN) high-performance computing initiative for the availability of high-performance computing resources and support. Authors are grateful to Dr. Thomas Humplik and Prof. Evelyn Wang (MIT) for the valuable discussions, as well as Alessio Bevilacqua for his support with molecular dynamics simulation.

References

[1] K. E. N'Tsoukpoe, H. Liu, N. Le Pierres, L. Luo, A review on long-term sorption solar energy storage, Renewable and Sustainable Energy Reviews 13 (9) (2009) 2385–2396.

[2] D. Aydin, S. P. Casey, S. Riffat, The latest advancements on thermochemical heat storage systems, Renewable and Sustainable Energy Reviews 41 (2015) 356–367.

[3] H. Garg, S. Mullick, A. Bhargava, Solar thermal energy storage, Springer, 1985.

[4] F. Kreith, J. F. Kreider, Principles of solar engineering, Washington, DC, Hemisphere Publishing Corp., 1978. 790 p. 1.

[5] K. Nielsen, Thermal energy storage: A state-of-the-art, Norway: Department of Geology and Mineral Resources Engineering, Trondheim (2003) 25.

[6] B. Zalba, J. M. Marín, L. F. Cabeza, H. Mehling, Review on thermal energy storage with phase change: materials, heat transfer analysis and applications, Applied thermal engineering 23 (3) (2003) 251–283.

[7] Y. Kato, Chemical energy conversion technologies for efficient energy use, in: Thermal energy storage for sustainable energy consumption, Springer, 2007, pp. 377–391.

[8] A. Hauer, Sorption theory for thermal energy storage, in: Thermal energy storage for sustainable energy consumption, Springer, 2007, pp. 393–408.

[9] T. Humplik, R. Raj, S. C. Maroo, T. Laoui, E. N. Wang, Framework water capacity and infiltration pressure of MFI zeolites, Microporous and Mesoporous Materials 190 (2014) 84–91.

[10] T. Humplik, J. Lee, S. O'Hern, B. Fellman, M. Baig, S. Hassan, M. Atieh, F. Rahman, T. Laoui, R. Karnik, et al., Nanostructured materials for water desalination, Nanotechnology 22 (29) (2011) 292001.

[11] A. Bertucci, H. Lülf, D. Septiadi, A. Manicardi, R. Corradini, L. De Cola, Intracellular delivery of peptide nucleic acid and organic molecules using zeolite-l nanocrystals, Advanced healthcare materials 3 (11) (2014) 1812–1817.

[12] E. Chiavazzo, M. Fasano, P. Asinari, P. Decuzzi, Scaling behaviour for the water transport in nanoconfined geometries, Nature communications 5 (2014) 4495.

[13] A. Gizzatov, J. Key, S. Aryal, J. Ananta, A. Cervadoro, A. L. Palange, M. Fasano, C. Stigliano, M. Zhong, D. Di Mascolo, A. Guven, E. Chiavazzo, P. Asinari, X. Liu, M. Ferrari, L. J. Wilson, P. Decuzzi, Hierarchically structured magnetic nanoconstructs with enhanced relaxivity and cooperative tumor accumulation, Advanced Functional Materials 24 (29) (2014) 4584–4594.

[14] M. Fasano, E. Chiavazzo, P. Asinari, Water transport control in carbon nanotube arrays, Nanoscale research letters 9 (1) (2014) 1–8.

[15] E. Chiavazzo, P. Asinari, Enhancing surface heat transfer by carbon nanofins: towards an alternative to nanofluids?, Nanoscale research letters 6 (1) (2011) 1–13.

[16] E. Chiavazzo, P. Asinari, Reconstruction and modeling of 3d percolation networks of carbon fillers in a polymer matrix, International Journal of Thermal Sciences 49 (12) (2010) 2272–2281.

[17] J. Janchen, D. Ackermann, H. Stach, W. Brosicke, Studies of the water adsorption on zeolites and modified mesoporous materials for seasonal storage of solar heat, Solar Energy 76 (1-3) (2004) 339–344.

[18] M. Fasano, M. B. Bigdeli, M. R. Sereshk Vaziri, E. Chiavazzo, P. Asinari, Thermal transmittance of carbon nanotube networks: Guidelines for novel thermal storage systems and polymeric material of thermal interest, Renewable & Sustainable Energy Reviews 41 (2015) 1028–1036.

[19] R. A. Shigeishi, C. H. Langford, B. R. Hollebone, Solar energy storage using chemical potential changes associated with drying of zeolites, Solar Energy 23 (6) (1979) 489–495.

[20] C. F. Parrish, R. P. Scaringe, D. M. Pratt, Development of an innovative spacecraft thermal storage device, in: IECEC'91; Proceedings of the 26th Intersociety Energy Conversion Engineering Conference, Volume 4, Vol. 4, 1991, pp. 279–284.

[21] A. Hauer, Thermal energy storage with zeolite for heating and cooling applications, in: Proceedings of 3rd Workshop of Annex, Vol. 17, 2002, pp. 1–2.

[22] Y. Lu, R. Wang, M. Zhang, S. Jiangzhou, Adsorption cold storage system with zeolite–water working pair used for locomotive air conditioning, Energy conversion and management 44 (10) (2003) 1733–1743.

[23] S. Henninger, F. Schmidt, H.-M. Henning, Water adsorption characteristics of novel materials for heat transformation applications, Applied Thermal Engineering 30 (13) (2010) 1692–1702.

[24] Y. Aristov, Concept of adsorbent optimal for adsorptive cooling/heating, Applied Thermal Engineering 72 (2) (2014) 166 – 175, special Issue: International Symposium on Innovative Materials for Processes in Energy Systems 2013 (IMPRES2013).

[25] K. Sanderson, Materials chemistry: Space invaders, Nature 448 (7155) (2007) 746–748.

[26] J. Kärger, In-depth study of surface resistances in nanoporous materials by microscopic diffusion measurement, Microporous and Mesoporous Materials 189 (2014) 126–135.

[27] J. Kärger, T. Binder, C. Chmelik, F. Hibbe, H. Krautscheid, R. Krishna, J. Weitkamp, Microimaging of transient guest profiles to monitor mass transfer in nanoporous materials, Nature Materials 13 (4) (2014) 333–343.

[28] R. Taylor, R. Krishna, Multicomponent mass transfer, Vol. 597, Wiley New York, 1993.

[29] R. Krishna, Diffusion in porous crystalline materials, Chemical Society Reviews 41 (8) (2012) 3099–3118.

[30] D. Tang, D. Kim, Study on the transport of water molecules under the geometry confinement of aquaporin-like nanopores, Applied Thermal Engineering 72 (1) (2014) 120–125.

[31] F. Schmidt, J. Luther, E. Glandt, Influence of adsorbent characteristics on the performance of an adsorption heat storage cycle, Industrial & Engineering Chemistry Research 42 (2003) 4910–4918.

[32] T. Humplik, R. Raj, S. Maroo, T. Laoui, E. N. Wang, Effect of hydrophilic defects on water transport in MFI zeolites, Langmuir 30 (22) (2014) 6446–6453.

[33] S. Curtarolo, G. L. Hart, M. B. Nardelli, N. Mingo, S. Sanvito, O. Levy, The high-throughput highway to computational materials design, Nature materials 12 (3) (2013) 191–201.

[34] S. Yip, M. P. Short, Multiscale materials modelling at the mesoscale, Nature materials 12 (9) (2013) 774–777.

[35] S. Hongois, F. Kuznik, P. Stevens, J.-J. Roux, Development and characterisation of a new MgSO 4- zeolite composite for long-term thermal energy storage, Solar Energy Materials and Solar Cells 95 (7) (2011) 1831–1837.

[36] F. Porcher, M. Souhassou, Y. Dusausoy, C. Lecomte, The crystal structure of a low-silica dehydrated nax zeolite, European journal of mineralogy (1999) 333–344.

[37] D. H. Olson, The crystal structure of dehydrated NaX, Zeolites 15 (5) (1995) 439–443.

[38] A. Di Lella, N. Desbiens, A. Boutin, I. Demachy, P. Ungerer, J.-P. Bellat, A. H. Fuchs, Molecular simulation studies of water physisorption in zeolites, Physical Chemistry Chemical Physics 8 (46) (2006) 5396–5406.

[39] P. Demontis, H. Jobic, M. A. Gonzalez, G. B. Suffritti, Diffusion of water in zeolites NaX and NaY studied by quasi-elastic neutron scattering and computer simulation, The Journal of Physical Chemistry C 113 (28) (2009) 12373–12379.

[40] C. Beauvais, X. Guerrault, F.-X. Coudert, A. Boutin, A. H. Fuchs, Distribution of sodium cations in faujasite-type zeolite: a canonical parallel tempering simulation study, The Journal of Physical Chemistry B 108 (1) (2004) 399–404.

[41] M. A. Granato, M. Jorge, T. J. Vlugt, A. E. Rodrigues, Diffusion of propane, propylene and isobutane in 13x zeolite by molecular dynamics, Chemical Engineering Science 65 (9) (2010) 2656–2663.

[42] J. L. Abascal, C. Vega, A general purpose model for the condensed phases of water: Tip4p/2005, The Journal of Chemical Physics 123 (23) (2005) 234505.

[43] B. Hess, C. Kutzner, D. Van Der Spoel, E. Lindahl, Gromacs 4: Algorithms for highly efficient, load-balanced, and scalable molecular simulation, Journal of chemical theory and computation 4 (3) (2008) 435–447.

[44] H. J. Berendsen, J. P. M. Postma, W. F. van Gunsteren, A. DiNola, J. Haak, Molecular dynamics with coupling to an external bath, The Journal of chemical physics 81 (8) (1984) 3684–3690.

[45] S. Nosé, A unified formulation of the constant temperature molecular dynamics methods, The Journal of Chemical Physics 81 (1) (1984) 511–519.

[46] P. E. Lopes, V. Murashov, M. Tazi, E. Demchuk, A. D. MacKerell, Development of an empirical force field for silica. Application to the quartz-water interface, The Journal of Physical Chemistry B 110 (6) (2006) 2782–2792.

[47] F. Cailliez, G. Stirnemann, A. Boutin, I. Demachy, A. H. Fuchs, Does water condense in hydrophobic cavities? A molecular simulation study of hydration in heterogeneous nanopores, The Journal of Physical Chemistry C 112 (28) (2008) 10435–10445.

[48] N. Desbiens, A. Boutin, I. Demachy, Water condensation in hydrophobic silicalite-1 zeolite: A molecular simulation study, The Journal of Physical Chemistry B 109 (50) (2005) 24071–24076.

[49] W. L. Jorgensen, J. Chandrasekhar, J. D. Madura, R. W. Impey, M. L. Klein, Comparison of simple potential functions for simulating liquid water, The Journal of Chemical Physics 79 (2) (1983) 926–935.

[50] B. Hess, H. Bekker, H. J. Berendsen, J. G. Fraaije, Lincs: a linear constraint solver for molecular simulations, Journal of Computational Chemistry 18 (12) (1997) 1463–1472.

[51] A. Gupta, S. Chempath, M. J. Sanborn, L. A. Clark, R. Q. Snurr, Object-oriented programming paradigms for molecular modeling, Molecular Simulation 29 (1) (2003) 29–46.

[52] E. F. Pettersen, T. D. Goddard, C. C. Huang, G. S. Couch, D. M. Greenblatt, E. C. Meng, T. E. Ferrin, UCSF Chimera-A visualization system for exploratory research and analysis, Journal of Computational Chemistry 25 (13) (2004) 1605–1612.

[53] M. P. Allen, D. J. Tildesley, Computer simulation of liquids, Oxford university press, 1989.

[54] J. Zhang, N. Burke, S. Zhang, K. Liu, M. Pervukhina, Thermodynamic analysis of molecular simulations of CO2 and CH4 adsorption in FAU zeolites, Chemical Engineering Science 113 (2014) 54–61.

[55] Y. Wang, M. D. LeVan, Adsorption equilibrium of carbon dioxide and water vapor on zeolites 5a and 13x and silica gel: pure components, Journal of Chemical & Engineering Data 54 (10) (2009) 2839–2844.

[56] T. Vlugt, E. Garcia-Perez, D. Dubbeldam, S. Ban, S. Calero, Computing the heat of adsorption using molecular simulations: the effect of strong coulombic interactions, Journal of Chemical Theory and Computation 4 (7) (2008) 1107–1118.

[57] O. Talu, R. L. Kabel, Isosteric heat of adsorption and the vacancy solution model, AIChE Journal 33 (3) (1987) 510–514.

[58] D. Olson, W. Haag, W. Borghard, Use of water as a probe of zeolitic properties: interaction of water with HZSM-5, Microporous and Mesoporous Materials 35 (2000) 435–446.

[59] C. E. Ramachandran, S. Chempath, L. J. Broadbelt, R. Q. Snurr, Water adsorption in hydrophobic nanopores: Monte Carlo simulations of water in silicalite, Microporous and mesoporous materials 90 (1) (2006) 293–298.

[60] S. Chen, R. Yang, Theoretical basis for the potential theory adsorption isotherms. the Dubinin-Radushkevich and Dubinin-Astakhov equations, Langmuir 10 (11) (1994) 4244–4249.

[61] F. Porcheron, P. Monson, M. Thommes, Modeling mercury porosimetry using statistical mechanics, Langmuir 20 (15) (2004) 6482–6489.

[62] M. Nagao, T. Morimoto, Differential heat of adsorption and entropy of water adsorbed on zinc oxide surface, The Journal of Physical Chemistry 73 (11) (1969) 3809–3814.

[63] K. Zhang, R. P. Lively, J. D. Noel, M. E. Dose, B. A. McCool, R. R. Chance, W. J. Koros, Adsorption of water and ethanol in MFI-type zeolites, Langmuir 28 (23) (2012) 8664–8673.